RSC Advances

This is an *Accepted Manuscript*, which has been through the Royal Society of Chemistry peer review process and has been accepted for publication.

Accepted Manuscripts are published online shortly after acceptance, before technical editing, formatting and proof reading. Using this free service, authors can make their results available to the community, in citable form, before we publish the edited article. This *Accepted Manuscript* will be replaced by the edited, formatted and paginated article as soon as this is available.

You can find more information about *Accepted Manuscripts* in the **Information for Authors**.

A Comprehensive Comparison of Bacterial and Fungal Aerobic Granules: Formation, Properties, Surface modification, and Biosorption of Metals

Li Wang[1, 5], Ya-yi Wang[5], Xiang Liu[2], Xiao-feng Chen[1], Duu-Jong Lee[3], Joo-Hwa Tay[4], Yi Zhang[2*], Chun-li Wan[2*]

[1]Center of Analysis and Measurement, Fudan University, Shanghai 200433, China
[2]Department of Environmental Science and Engineering, Fudan University, 220 Handan Road, Yangpu District, Shanghai 200433, China
[3]Department of Chemical Engineering, National Taiwan University of Science and Technology, Taipei 106, Taiwan
[4]Department of Civil Engineering, University of Calgary, Calgary, Canada
[5]State Key Laboratory of Pollution Control and Resource Reuse Foundation, School of Environmental Science and Engineering, Tongji University, Shanghai, China

* Co-corresponding authors:

Yi Zhang: zhang-yi@fudan.edu.cn, 86-21-55664354

Chun-li Wan: hitwan@163.com, 86-21-65642781

Abstract: Aerobic granules, a relatively new form of microbial aggregate, can be formed with bacteria or fungi as the dominant population, depending on operational conditions. In this study, a comprehensive comparison is conducted between these two kinds of granules. Bacterial granules (BG) were formed after 3 weeks cultivation, and exhibited settling velocity and ash content of 5.6 cm s^{-1} and 24%, respectively. In

contrast, fungal granules (FG) cultivation took only 5 days, and their settling velocity

and ash content were 45% and 22% of BG, respectively. BG and FG selectively

enriched calcium and potassium, respectively, and these elements were replaced by

iron upon Fe(III) modification. Original BG had 7 times bigger surface area and 9

times higher pore volume than FG, but Fe(III) modification reversed the trend.

Original and modified granules were used as biosorbents for removal of Zn(II), Cu(II),

Ni(II) and $Sb(OH)_6^-$ under various pH levels. The original granules removed the

cations efficiently (BG better than FG), but had no affinity for Sb(V) under all pH.

Fe(III) modification significantly enhanced Sb(V) removal by both granules, with the

best performance achieved under pH 3.4. FG, though had lower Fe loading, exhibited

comparable ultimate Sb(V) adsorption capacity to BG (111 vs. 125 mg g^{-1}), and 3

times higher initial adsorption rate. In addition, FG was more stable under higher pH

and showed better adsorption performance under pH>4.3. Pseudo-second-order

kinetics and Langmuir isotherm model described the adsorption processes well for

both kinds of modified granules, which proved to be good biosorbents.

Key words: Aerobic granules; Bacterial; Fungal; Surface modification; Biosorption;

Metal removal

1. Introduction

Aerobic granule is a promising wastewater treatment technology, which can

efficiently remove organics, nitrogen, phosphorus, and toxic substances.[1] Mature granules are usually compact in structure and high in density, and harboring various functional populations like heterotrophic, nitrifying, denitrifying and phosphorous-accumulating bacteria.[2] However, researchers have discovered that some operation conditions could lead to overgrowth of filamentous microorganisms in aerobic granules.[3-7] For example, carbohydrates like glucose and citric acid, and some other readily biodegradable organics are believed to favor the growth of the filamentous microorganisms; acidic pH could also shift the structure of the microbial community in the granules towards filamentous growth. Some of these filamentous cells were later confirmed to be fungi populations.[6,7] The filamentous granules formed are characterized by their loose structure and low density, which can cause severe biomass washout from reactors. Therefore, fungal granules are often considered useless in practice, and detrimental to process stability.

However, some recent studies have proposed a potential application for the fungal granules, as they had exhibited considerable biosorption capacity, especially after surface modification.[7] Biosorption is an eco-friendly and cost-effective way to removal heavy metals from aqueous medium,[8] and aerobic granule has been investigated as a promising biosorbent due to its excellent settleability and compact structure.[9] Up to now, mainly aerobic granules had been applied, while only a few have dealt with biosorption by both bacterial and fungal granules, utilizing Fe(III) imbedding as a surface modification method. Biosorption of Sb(V) onto Fe-modified bacterial granules was first experimented, and the kinetics, isotherm, thermodynamic,

influencing factors and adsorption mechanism were studied in detail.[10,11] Moreover, the microbial community of fungal granules and use of Fe(III)-modified fungal granules for Sb(V) biosorption were also briefly discussed.[7]

These studies, though rigorous and detailed, are somewhat isolated and cannot provide a full picture of these two kinds of granules. Therefore in this work, it is intended that a comprehensive comparison should be made, based on previous and new results, to give an overview of the characteristics and applicability of bacterial and fungal aerobic granules. The objectives of this work are: **I)** to study in detail the differences in the cultivation conditions, morphology, physical structure, and chemical composition of bacterial and fungal granules; **II)** to perform Fe(III) surface modification on these granules, and to investigate the respective changes in their properties; **III)** using Cu(II), Zn(II) and Ni(II) as model cations to test the biosorption capacities of unmodified granules. **IV)** using Sb(V) as the model oxyanion and kinetic modeling as tools, to study the adsorption capacity, velocity, and maximum quantity of modified granules. Finally a comprehensive appraisal on the bacterial and fungal granules is presented, which has not been attempted before, and would provide valuable information in both fundamental research and practical applications.

2. Experimental

2.1 Cultivation and preparation of aerobic granules

Two identical sequencing batch reactors (SBRs), i.e., R_1 and R_2 were used to cultivate bacterial and fungal granules, respectively. Activated sludge obtained from a

nearby domestic wastewater treatment plant was inoculated into the reactors for granule cultivation. They were both operated at 4 h cycles, with air pumped through diffusers at the bottom (volumetric flow rate 5 L min^{-1}). Each cycle included 3 min filling, 227 min aeration and settling, 5 min effluent decanting, and 5 min idling. The settling time was reduced from 30 min to 1 min for R_1, but was fixed at 5 min for R_2. R_1 was fed with a synthetic wastewater with the composition of NH_4Cl (0.2 g L^{-1}), KH_2PO_4 (0.66 g L^{-1}), $NaHCO_3$ (0.013 g L^{-1}), $MgSO_4 \cdot 7H_2O$ (0.025 g L^{-1}), $CaCl_2$ (0.03 g L^{-1}), $FeSO_4 \cdot 5H_2O$ (0.02 g L^{-1}), peptone (0.4 g L^{-1}), and yeast extract (0.25 g L^{-1}). The synthetic wastewater for R_2 contained the same components, except for KH_2PO_4 (0.2 g L^{-1}), peptone (0.04 g L^{-1}), and no yeast extract. Carbon sources for R_1 were sodium acetate and propionate at a combined chemical oxygen demand (COD) concentration of 1000–3000 mg L^{-1} in the influent, while glucose (COD concentration 1000 mg L^{-1}) was provided for R_2 as the sole carbon source. These differences in the wastewater composition aimed to promote the formation of different granules. The reduced KH_2PO_4 concentration resulted in lower buffering capacity, which, combined with the lower COD loading in R_2, could promote the growth of fungal granules. After granule formation, both granules were harvested from the SBRs, and washed with MilliQ water three times before tests.

2.2 Surface modification by Fe(III)

The granules were modified using the same method as reported in previous work.[7,11] Specifically, bacterial or fungal granules (25 g on wet basis) were incubated

5

with 250 mL 0.1 M $FeCl_3$ solution. The suspension was continuously shaken on an orbital shaker for 24 h at 35 °C, pH 2.0 and 160 rpm. Subsequently, the Fe-modified granules were collected and repeatedly washed with MilliQ water until no Fe(III) can be detected in the supernatant, then stored in tap water at 4 °C until use. The original aerobic granules were designated as OAGS-B (bacterial) and OAGS-F (fungal), and the modified aerobic granules MAGS-B and MAGS-F, respectively.

2.3 Adsorption tests

Cu(II), Zn(II) and Ni(II) were used as the target metal cations for biosorption experiments by unmodified granules. The standard stock solutions of these ions (1000 mg L^{-1}) were prepared by dissolving $CuSO_4$, $ZnCl_2$ or $NiSO_4$ in MilliQ water, which were further diluted and its pH adjusted with 0.1 M HCl. OAGS-B or OAGS-F of 0.5 g (wet basis, average water content 94.2±0.2%) were mixed with 10 mg L^{-1} solution of each ion, and the removal was studied under pH 1.9, 2.6, 3.4, 4.8, 6.5 and 7.6.

Sb(V) was applied as the model oxyanionic metal for adsorption tests with both the original and modified granules. The Sb(V) standard stock solution of 1000 mg L^{-1} was prepared by dissolving $KSb(OH)_6$ in MilliQ water, and was further diluted to the desired concentrations. 0.1 M HCl or NaOH was added to adjust pH in the range of 2 to 11.4 to study the pH effect. For adsorption kinetics, initial Sb(V) concentrations of 20, 60 and 100 mg L^{-1} were used. For the adsorption isotherms, the concentrations varied from 10 to 500 mg L^{-1}, and the thermodynamics analysis was conducted under temperatures from 10 °C to 45 °C. The contact time for all the tests was 300 min.

In the adsorption tests, the supernatant of the solution was collected at fixed time intervals and centrifuged at 10000 rpm for the subsequent measurement of metal concentrations. The adsorption quantity, q_t was expressed as: $q_t = (C_0 - C_e)*v/m$, where C_0 and C_e are the initial and equilibrium concentrations (mg L^{-1}), respectively; v represents the solution volume (L), and m is the dried weight of the sorbent. The amount of Sb adsorbed by the flask was measured as the blank, and was found to be negligible. All tests were performed in triplicate, and all the results are shown as mean values with the error bars as the standard deviation.

2.4 Sampling and analytical methods

Various physical and chemical characteristics of the granules were studied, including their morphology by digital camera imaging and scanning electron microscopy (SEM) observation, metal composition, surface area, functional groups, and microbial population. For electron microscopy, granules were sequentially dehydrated by a serial of ethanol solutions of increasing concentrations and dried overnight, followed by coating with aurum and observation by a Philips XL30 electron microscope. Microanalysis by transmission electron microscopy (TEM) equipped with energy-dispersive X-ray spectrometry (EDS) was conducted on a JEOL JEM2011 instrument. The surface areas of the samples were determined with a BET (Brunauer–Emmett–Teller) system (Quadrasorb SI instrument) from the nitrogen sorption isotherm at -196 °C. Functional groups were studied by fourier transformation spectroscopy (FTIR, Nicolet Nexus-470), which was performed on

KBr pellets pressed from the mixture of 1 mg dried granules and 100 mg spectrometry grade KBr under vacuum. X-ray diffraction (XRD) analysis was conducted on a Bruker D8 Advance X-ray diffractometer using nickel-filtered Cu Kα radiation at 40 kV and 40 mA. The concentrations of Sb and other common metals were analyzed by an Inductively Coupled Plasma Atomic Emission Spectrometer (ICP-AES, HITACHI P-4010). The concentrations in the solutions were directly measured, while those in the biomass were determined after its digestion and dissolution in acid. The concentrations of Cu, Zn and Ni were measured using flame atomic absorption spectroscopy (AAS, HITACHI Z-5000).

2.5 Adsorption models and mechanism

The kinetics, isotherms and thermodynamics were studied using widely accepted models, including Pseudo-first-order and Pseudo-second-order kinetics, and Langmuir and Freundlich isotherms. The thermodynamic parameters of entropy ($\triangle S$), enthalpy ($\triangle H$) and Gibbs free energy ($\triangle G$) were also obtained. The detailed models, parameters and calculations are shown in the supplementary materials (Table S2-S4).

3. Results and discussion

3.1 Granule cultivation and morphology characteristics

Bacterial granules of size 3-5 mm were formed after 20 days in R_1, the progress of which is showed in Fig. S1. During cultivation, the morphology of the biomass changed from highly dispersed flocs to structure-compact aggregates, and the COD

removal efficiency was usually higher than 98%. Further study indentified various bacteria as the dominating populations.[12] In contrast, filamentous granules with fluffy surface were observed in R_2 after only 5 days, and the changes in biomass morphology can be seen in Fig. S2. The size of the filamentous granules ranged from 1 to 7 mm, and their COD removal capacity was comparable to those in R_1. These granules were found to be dominated by one fungal species, *Geotrichum fragran.*[7] During the aeration phrase in a cycle, the pH increased from 7 to 8.5 in R_1, but decreased from 7 to 4.5 in R_2. The different carbon sources used in the cultivation very likely caused the different trends of pH change, by producing various intermediates during substrate degradation. Glucose in R_2 could be degraded to pyruvate following a glycolytic pathway, and further transformed into volatile fatty acids, which would lead to an acidic condition.[6] Moreover, KH_2PO_4 content in R_2 was significantly lower, resulting in a weaker buffer capacity. These factors in combination contributed to the sustained low pH in R_2, which in turn influenced the microbial community structure of the granules. It has been reported that pH was the determining parameter in the type of granules formed, and low pH caused the overgrowth of filamentous microorganisms and formation of fungal granules.[6]

Significant differences in the morphology were observed between OAGS-B and OGSB-F, as shown in Fig. 1(A) and (F). OAGS-B had light-yellow surface and irregular shape, while OGSB-F was white and near-spherical. Further observation of the granules surface suggested that OAGS-B had compact structure, and OGSB-F was loose, with abundant mycelia entangled with each other (Fig. 1(C) and (H)). Some

physicochemical characteristics are shown in Table 1. Sludge volume index (SVI)

reflects the sludge settling ability, and the SVI of OAGS-F was twice that of OGSB-B.

In addition, the settling speed of OGSB-B was 124 % higher than that of OAGS-F,

which indicated that OAGS-F settled more slowly, and when settled, formed less

compact sludge bed. This is in accordance with the fluffy structure of the fungal

granules. The two kinds of granules had similar moisture contents, but the ash content

in OGSB-B (24 %) was significantly higher than that in OAGS-F (5.2 %). It seemed

that bacterial granules were more inclined to incorporate mineral elements into their

structure. It was suggested that addition of Ca^{2+} or Mg^{2+} enhanced aerobic

granulation,[13] which is in agreement with the higher ash content and settling ability

found with OAGS-B in this study. However, if, and how does the lower ash content

correlate to the formation and properties of fungal granules requires further study, as

the same Ca^{2+} and Mg^{2+} concentrations were provided in the cultivation medium.

3.2 Fe(III) modification on the granules

Surface modification is a practical technique for metal removal by biosorption, and

iron is a promising modification agent, as it is cheap and non-toxic.[14] In this study, the

granules were subjected to modification by Fe(III), in the hope of expanding their

applicability in biosorption. Both granules exhibited color change to brownish after

Fe(III) embedding, but their general shapes seemed to be unchanged, as shown in Fig.

1(B) and (G). However, different pH significantly affected the integrity of the

modified granules and the iron speciation on their surface, the details of which were

described in previous work.[7,11] In short, strong acid led to the dissolution of iron hydro(oxide) on the surface, and disintegration of MAGS-B was observed under strong alkaline conditions. However, the integrity of MAGS-F seemed to be unaffected by high pH, though the change of the iron speciation was similar.

Finer details on the granules' surface were observed using SEM and TEM with EDS. OAGS-B consisted of cocci and bacilli of size 0.5-2 μm closely grouped together, while OAGS-F was made up of intertwined mycelia with the diameter of around 2 μm, and presented a more loose and hollow structure (Fig. 1(D) and (I)). After FeCl₃ treatment, the surface of the granules became coarse and wrinkled and nano-precipitates were observed (Fig. 1(E) and (J)), which are also seen in the TEM images (Fig. 2(B) and (D)). EDS spectra confirmed the particles to be iron compound. The spectra also showed that OAGS-B and OAGS-F enriched elements Ca and K, respectively, which were replaced by iron after Fe(III) modification (Fig. 2(E)-(H)).

3.3 Further characterization of the granules' physiological properties

3.3.1 Metal composition

As mentioned in section 3.2, it was possible that the granules selectively enriched certain metal elements in the biomass. To further investigate this phenomenon, elemental analysis of some common metals was conducted on both granules before and after Fe(III) modification and the results are summarized in Table S1.[7,11] Elements Ca and K were selectively enriched in OAGS-B and OAGS-F, respectively, with the corresponding contents of 8.8 % and 2.5 %. The iron contents in OAGS-B and

OAGS-F were insignificant. However after Fe(III) modification, they increased to 5.9 %

and 1.6 % for MAGS-B and MAGS-F (0.059 and 0.016 mg mg granule^{-1}),

respectively. This indicated that Fe was indeed taken up by the granules, and the BG

had almost 4 times Fe loading capacity of FG. Meanwhile, a sharp decrease in all

other common metals (K, Na, Ca, and Mg) was observed, one reason of which could

be that iron modification was accompanied by the hydrolysis of $FeCl_3$. The resultant

acidic condition in the solution would dissolve these metals in the granules. Ion

exchange between Ca/K and Fe could also play a role.

3.3.2 Analysis of surface area

Specific surface area is an important parameter reflecting the adsorption capacity of

an adsorbent. The granules' surface area was analyzed by BET, and the results are

presented in Table 2. OAGS-B and OAGS-F had specific surface areas of 65.4 and 9.1

m^2 g^{-1}, respectively, which changed to 8.52 and 29.7 m^2 g^{-1} after modification.

Accordingly, the pore volume of BG decreased from 0.196 to 0.029 mL g^{-1}, whereas

that of FG increased from 0.021 to 0.054 mL g^{-1}. This significant difference could

probably be attributed to the distinct physical structures of the granules. Upon contact

with $FeCl_3$, bacterial granules shrank slightly, which might have prevented foreign

ions permeating into their interior, and formation of iron-precipitate might further

block the pores. These factors in combination resulted in a decrease in surface area

and pore volume. Similar results were also found in a study of activated carbon

modified with iron to be used as adsorbent for arsenate removal.[15] However, OAGS-F

mainly contained long intertwined mycelia, which corresponded to relative small

surface area. The nano-particle precipitation onto the mycelia in turn increased the specific surface area, which might enhance their adsorption capacity

3.3.3 Analysis of granule surface by FTIR and XRD

Functional groups analysis was conducted by FTIR, and the results are shown in Fig. 3 with all the major groups marked. The bands in the region of 3200 to 3600 cm^{-1} reflect the overlapping of stretching vibration of OH and NH, indicating the presence of hydroxyl and amine groups on both the granules' surface. The bands at 2925 and 2856 cm^{-1} are indicative of asymmetric and symmetric stretching vibration of CH_2, respectively. The band at 1261 cm^{-1} results from the deformation vibration of C=O, while that at 1056 cm^{-1} is attributed to the stretching vibration of OH from polysaccharides [9]. After Fe(III) modification, for both granules the band at 3399 cm^{-1} shifted to 3321 and 3367 cm^{-1}, while that at 1056 cm^{-1} shifted to 1076 and 1065 cm^{-1}, respectively. However, hardly any shifts were observed for the bands 1261, 2925 and 2856 cm^{-1}. These results indicated that hydroxyl group on the biomass surface played an important role in Fe(III) modification, while the effect of other functional groups including amine, CH_2 and C=O was not as significant. XRD analysis was also performed to indentify the properties of Fe-precipitates formed on the biomass. However, no significant diffraction peak was observed (data not shown). This suggested that either the content of iron hydro(oxide) was not high enough to be detected, or the iron-precipitates formed was amorphous, or both. Based on the collective results, the mechanisms of Fe(III) modification were proposed in Fig. S3, where ion-exchange with Fe^{3+} and iron hydroxides complexation with the surface

functional groups (most likely hydroxyl) in the extracellular polymers were the major

contributing factors.

3.4 Adsorption tests with Cu(II), Zn(II) and Ni(II)

Most of heavy metals exist in the form of cations in aqueous media, and therefore

the aerobic granules, usually negatively charged (point of zero charge, pH_{pzc} = 2.4),[16]

are often used to remove cationic metals.[17,18] In this study, several common and toxic

metals, i.e. Cu(II), Zn(II) and Ni(II) were selected as model cations to briefly test the

adsorption capacity of original granules. To avoid precipitation, pHs from 1.9 to 7.6

were selected, and the respective removal efficiencies are shown in Fig. 4. In almost

all cases, OAGS-B had much higher capacity than OAGS-F, the only exceptions

being Cu and Ni under pH 1.9. Under other pH, the removal by the former for all 3

ions was 1 to 4 times higher than that by the latter. This was in accordance with the

higher surface area of OAGS-B. In addition, the elevated Ca and Mg levels in

OAGS-B might also contribute through ion exchange with the cations, which was

confirmed in a previous study of Sr(II) removal by aerobic granules.[19] On the other

hand, the removal of the tested cations was strongly dependant on solution pH for

both granules. It has been reported that pH is an important factor that influences both

metal and cell surface chemistry.[20] Aerobic granules would be protonated and

positively charged under pH below its pH_{pzc}, therefore the adsorption of cations would

be inhibited under low pH due to electrostatic repulse between metal ions and the

biomass. In contrast, pH ranging from 3.4 to 7.6 resulted in much better adsorption

performance by both granules. In terms of individual metals, Cu(II) and Zn(II) exhibited significantly better removal effect than Ni(II), the reason of which is not clear.

3.5 Adsorption tests with Sb(V)

Heavy metals can also exist in the form of oxyanion, the examples of which include Sb(V), As(V), and Cr (VI). Among them, Antimony (Sb) is widely applied in a variety of industrial activities, and considered as a pollutant of priority interest by various agencies.[21,22] Sb(V) was found to be dominant and stable in oxygenated systems, with oxyanion $Sb(OH)_6^-$ as the common form.[23] Therefore, Sb(V) was selected as the model oxyainon in this study to investigate the adsorption capabilities of the bacterial and fungal granules, both before and after Fe(III) modification.

3.5.1 Effect of pH on the adsorption capacities of the granules

Sb(V) removal by OAGS and MAGS was compared under 3 different pH, and the respective time courses are shown in Fig. 5. OAGS showed no affinity for Sb(V) regardless of pH. When modified by Fe(III), removal efficiencies were significantly improved for both granules. The highest improvement occurred under pH 3.4, with both removal percentages higher than 99 % at 300 min, but MAGS-F achieved the effect much faster (at around 50 min) than MAGS-B (approx. 125 min). In addition, modified granules exhibited different sensitivities to pH. At pH 2.0 or 10.4, MAGS-B removed 60 or 6 % of the initial 20 mg L^{-1} Sb(V), respectively, while the percentages were 40 or 23 % for MAGS-F. Therefore MAGS-F showed higher and faster removal

than MAGS-B under pH 3.4 and 10.4, while MAGS-B performed better at pH 2.0

The pH effect was studied in more details for MAGS and the results are summarized in Fig. 6. Sb(V) could exist as a negatively charged complex in pH from 2 to 11,[24] which was the range tested. Both MAGS-B and MAGS-F exhibited a similar trend with pH change. The pH 3.4 was found to be optimal, with removal percentages around 99 % for both granules. Strong acidic or alkaline conditions negatively affected the removal efficiency, and in general the effect of high pH was more pronounced. MAGS-B and MAGS-F exhibited different susceptibility to acidic/alkaline environments, and the threshold seemed to be around 4.3. Below that pH, MAGS-B showed higher efficiency than MAGS-F, while the opposite was observed under neutral and alkaline conditions. This agreed well with the phenomenon described in section 3.2, that the structural stability of MAGS-B was greatly reduced under higher pH, while that of MAGS-F was not much affected.

The pH effect could be the result of the interactions of several mechanisms. On one hand, the granules would be protonated and positively charged under pH lower than pH_{pzc}, promoting $Sb(OH)_6^-$ removal. Nevertheless, pH 2 might lead to dissolution of the bonded iron, thus weakening the adsorption. On the other hand, the granules could be negatively charged in alkaline solution due to the existence of abundant OH^-, which would result in electrostatic repulsion with the oxyaion $Sb(OH)_6^-$. As pH 3.4 gave the best performance for both granules, it was applied in all later experiments.

3.5.2 Adsorption kinetics

As aforementioned, fungal granules exhibited faster removal under certain

16

conditions, therefore the adsorption kinetics were further studied under several initial concentrations, and the comparison is shown in Fig. S4. Higher initial concentrations resulted in higher adsorption amounts for both granules, possibly because the ratio of initial Sb(V) quantity to available adsorption sites was high at higher initial concentrations,[25] providing bigger driving force. The equilibrium adsorption quantities were found to be 33.9, 85.9 and 130 mg g^{-1} for MAGS-F, and 36.6, 102, and 146 mg g^{-1} for MAGS-B at initial Sb(V) concentrations of 20, 60, and 100 mg L^{-1}. Therefore MAGS-B had slightly higher ultimate adsorption capacity, but MAGS-F showed faster initial adsorption in all cases. For MAGS-F, 53.8, 59.8 and 61.2% of the equilibrium quantity were accomplished within 5 min at 20, 60 and 100 mg L^{-1}, respectively, which was almost twice as much as that of MAGS-B.

The experimental data were further fitted with two classic kinetic models to better understand the mechanisms, and the respective parameters are listed in Table S2. Pseudo-second-order model could better describe Sb(V) adsorption by both granules, with the correlation coefficients higher than 0.998 in all cases, and the calculated equilibrium adsorption quantities agreed well with the experimental data. Parameters k_2, h and $t_{1/2}$ represent the sorption rate, initial sorption rate and half-adsorption time, respectively, in this model. They were used to evaluate the adsorption kinetics, and the results are compared in Fig. 7. At the same initial concentrations, both k_2 and h of MAGS-F were significantly higher than those of MAGS-B. The main reason could be the physical structure of the granules. MAGS-F had larger surface area, with more active adsorption sites exposed to Sb(V), thus promoting film and pore diffusion

within a short time. Correspondingly, the calculated $t_{1/2}$ ranged from 4.8 to 6.3 min for MAGS-F, much shorter than those of MAGS-B (16 to 20 min).

3.5.3 Adsorption isotherm

The equilibrium adsorption data were fitted with Langmuir and Freundlich isotherm models, the detailed discussions of which had been presented in previous studies.[7,10] In this study, the respective results are listed in Table S3 for better comparison. Generally, the data for both MAGS-B and MAGS-F could be better described by the Langmuir model, with the correlation coefficients (r^2) of 0.987 and 0.997, respectively. It indicated that Sb(V) adsorption by both kinds of granules was likely monolayer sorption. The theoretical maximum adsorption quantities calculated from the Langmuir model were 125 and 111 mg g^{-1} for MAGS-B and MAGS-F, respectively. It agreed well with the experimental data, that the fungal granules have a comparable Sb(V) removal capacity, in spite of its lower iron loading.

3.5.4 Thermodynamics analysis

The thermodynamic analysis of the adsorption process by MAGS-B has been discussed before,[10] and that of MAGS-F was conducted in this study. The respective parameters are listed in Table S4, which indicated that MAGS-B and MAGS-F had similar thermodynamic characteristics. The enthalpy change (ΔH) values were found to be positive, indicating the adsorption was endothermic, and higher temperature would favor the process. Moreover, in the temperature range of 10 to 45 °C, the negative values of Gibbs free energy (ΔG) implied that Sb(V) adsorption by both granules were spontaneous.

3.5.5 Adsorption mechanisms

The mechanism of Sb(V) adsorption by MAGS-B has been investigated in details before. [10,11] In addition, FTIR data were obtained for the modified granules after Sb(V) adsorption in this study, and the results are shown in Fig. 3. Comparing the profiles of the modified granules before and after adsorption, it can be seen that bands at 3200-3600 cm^{-1} and 1056-1076 cm^{-1} have shifted. More specifically for the modified bacterial granules, the band at 3321 cm^{-1} shifted to 3388 cm^{-1}, and that at 1076 cm^{-1} to 1066 cm^{-1}. For modified fungal granules the corresponding changes were 3367 cm^{-1} to 3393 cm^{-1} and 1065 cm^{-1} to 1058 cm^{-1}. In fact, Sb(V) adsorption resulted in FTIR profiles that were closer to the original granules, and the main functional groups affected seemed to be OH related. As OH was the major functional group involved in Fe(III) modification, it was possible that Sb(V) interacted with the Fe-OH complex on granules surface and somehow changed the FTIR profiles. Moreover, the shifts were more dramatic for the bacterial granules (3399-3321-3388 and 1056-1071-1066 cm^{-1}) than the fungal granules (3399-3367-3393 and 1056-1065-1058 cm^{-1}), but the reason is unclear.

Based on previous results and the new data presented in this study, the mechanism of Sb(V) removal by Fe(III) modified aerobic granules is proposed as a combination of electrostatic attraction, ion-exchange, and surface complexation. First, iron modification causes precipitation of ferric hydroxides on granule surface (>Fe-OH). At low pH, the surface of the modified granules could be protonated to

form $>Fe\text{-}OH_2^+$, which are positively charged. The positively charged surface could then easily attract the negatively charged Sb(V) species and form out-sphere complex [$>Fe\text{-}OH_2^+ \cdot Sb(OH)_6$] through electrostatic attraction and ion-exchange. Subsequently when the modified granules were ashed after Sb adsorption, dark insoluble residue was observed. It was then deducted that inner-sphere complex ($>Fe\text{-}O\text{-}Sb$) was formed through dehydration, resulting in more stable chemical bonds and residues insoluble in strong acid.[10] Furthermore, other positively charged iron species, such as $Fe(OH)^{2+}$, $Fe_2(OH)_2^{4+}$, $Fe_3(OH)_4^{5+}$ could also be combined with the granules surface,[11] which would enhance Sb(V) removal furthermore.

3.6 Biosorbent assessment

Generally, the adsorption performance of a biosorbent for metal removal is determined by multiple factors, including ease and cost of preparation, settleability and stability, sorption rate and capacity, and potential environmental impact. The maximum adsorption capacities of several organic and inorganic adsorbents for $Sb(OH)_6^-$ are listed in Table 3 for comparison. The modified aerobic granules used in this study showed higher capacity than most adsorbents listed, and the process was usually completed in a shorter time. Therefore in terms of adsorption capacity and separation efficiency, the modified aerobic granules are potentially good biosorbents.

A conclusion of the various aspects of the two kinds of granules is shown in Table S5. OAGS-B, with compact structure and high density, had better settleability in the aqueous solution. It had larger surface area and pore volume, and higher iron loading

after Fe(III) modification. Bacterial granules also showed higher removal capacity for the cationic metals tested while unmodified, and a greater ultimate adsorption quantity for oxyanionic metals, $Sb(OH)_6^-$ after modification. However, longer time was needed for their cultivation, and their adsorption equilibrium for Sb(V) was achieved more slowly. In contrast, the fungal granules could be formed in shorter time from activated sludge. Fe(III) modified fungal granules had higher surface area despite their lower iron loading, and their sorption rate for Sb(V) was higher especially in the initial phase. Therefore fungal granules utilized the modifying agent Fe(III) more efficiently. In addition, fungal granules exhibited higher structural strength under alkaline conditions, which resulted in their better performance at higher pH. In a word, the bacterial and fungal granules have their respective advantages and disadvantages in cultivation, properties and performances in metal bisorption. It is the first time that the advantages of fungal aerobic granules are systematically investigated, and a comprehensive comparison conducted between the bacterial and fungal granules, which could be of both research and practical interest.

Acknowledgement:

References:

1. D. J. Lee, Y. Y. Chen, K. Y. Show, C. G. Whiteley and J. H. Tay, *Biotechnol. Adv.*, 2010, **28**, 919–934.

2. S. S. Adav, D. J. Lee, K. Y. Show and J. H. Tay, *Biotechnol. Adv.*, 2008, **26**, 411–423.

3. Y. Liu and Q. S. Liu, *Biotechnol. Adv.*, 2006, **24**, 115–127.

4. Y. M. Zheng, H. Q. Yu, S. J. Liu and X. Z. Liu, *Chemosphere*, 2006, **63**, 1791–1800.

5. Y. Liu, and J. H. Tay, *Biotechnol. Adv.*, 2004, **22**, 533–563.

6. C. Wan, X. Yang, D. J. Lee, Q. Zhang, J. Li and X. Liu, *Appl. Microbiol. Biot.*, 2014, **98**, 8389–8397.

7. C. Wan, L. Wang, D. J. Lee, Q. Zhang, J. Li and X. Liu, *J. Taiwan Inst. Chem. E.*, 2014, **45**, 2610–2614.

8. Y. S. Yun, D. Park, J. M. Park and B. Volesky, *Environ. Sci. Technol.*, 2001, **35**, 4353–4358.

9. H. Xu and Y. Liu, *Sep. Purif. Technol.*, 2008, **58**, 400–411.

10. L. Wang, C. Wan, Y. Zhang, D. J. Lee, X. Liu, X. F. Chen and J. H. Tay, *J. Hazard. Mater.*, 2015, **284**, 43–49.

11. L. Wang, C. Wan, D. J. Lee, X. Liu, Y. Zhang, X. F. Chen and J. H. Tay, *Bioresource Technol.*, 2014, **158**, 351–354.

12. C. Wan, P. Zhang, D. J. Lee, X. Yang, X. Liu, S. Sun and X. Pan, *Bioresource Technol.*, 2013, **146**, 330–335.

13.   L. Liu, D. W. Gao, M. Zhang and Y. Fu, *J. Hazard. Mater.*, 2010, **181**, 382–387.

14.   M. Aryal, M. Ziagova and M. Liakopoulou-Kyriakides, *Chem. Eng. J.*, 2011, **169**, 100–106.

15.   A. V. Vitela-Rodriguez and J. R. Rangel-Mendez, *J. Environ. Manage.*, 2013, **114**, 225–231.

16.   F. Sun, W. L. Sun, H. M. Sun and J. R. Ni, *Chem. Eng. J.*, 2011, **172**, 783–791.

17.   L. H. Gai, S. G. Wang, W. X. Gong, X. W. Liu, B. Y. Gao and H. Y. Zhang, *J. Chem. Technol. Biot.*, 2008, **83**, 806–813.

18.   Y. Liu, H. Xu, S. F. Yang and J. H. Tay, *J. Chem. Technol. Biot.*, 2004, **79**, 982–986.

19.   L. Wang, X. Liu, X. Chen, D. J. Lee, J. H. Tay, Y. Zhang and C. Wan, *J. Radioanal. Nucl. Che*m., 2015, **306**, 193–202.

20.   S. Durmaz-Sam, N. A. Sayar, A. Topal-Sarikaya and A. A. Sayar, *Bioproc. Biosyst. Eng.*, 2011, **34**, 997–1005.

21.   O. D. Uluozlu, A. Sari and M. Tuzen, *Chem. Eng. J.*, 2010, **163**, 382–388.

22.   A. G. Leyva, J. Marrero, P. Smichowski and D. Cicerone, *Environ. Sci. Technol.*, 2001, **35**, 3669–3675.

23.   F. H. Sun, F. C. Wu, H. Q. Liao and B. S. Xing, *Chem. Eng. J.*, 2011, **171**, 1082–1090.

24.   J. Xi, M. He and C. Lin, *Environ. Earth Sci.*, 2010, **60**, 715–722.

25.   K. A. Krishnan, K. Sreejalekshmi and R. Baiju, *Bioresource Technol.*, 2011, **102**, 10239–10247.

26. B. K. Biswas, J. Inoue, H. Kawakita, K. Ohto and K. Inoue, *J. Hazard. Mater.*, 2009, **172**, 721–728.

27. X. Guo, Z. Wu, M. He, X. Meng, X. Jin, N. Qiu and J. Zhang, *J. Hazard. Mater.*, 2014, **276**, 339–345.

Table 1 Physicochemical characteristics of the original bacterial and fungal aerobic granules.

	SVI	Settling velocity	Moisture content	Ash content
	$(mL\ g^{-1})$	$(cm\ s^{-1})$	(%)	(%)
OAGS-B (R_1)	48	5.6	92	24
OAGS-F (R_2)	74	2.5	93	5.2

Table 2 Analysis of the granules' surface area and pore volume by BET before and

after Fe(III) modification.

	Specific surface area ($m^2\ g^{-1}$)	Pore volume ($mL\ g^{-1}$)	Pore size (nm)
OAGS-B	65.4	0.196	12.38
Fe-MAGS-B	8.52	0.029	14.81
OAGS-F	9.10	0.021	10.81
Fe-MAGS-F	29.7	0.054	6.97

Table 3 Comparison of maximum adsorption capacities of Sb(V) onto various adsorbents.

Adsorbent	Adsorbate	pH	Biomass dose (g L^{-1})	Temperature (℃)	Contact time (h)	Maximum sorption capacity (mg g^{-1})	Reference
MAGS(F)	Sb(V)	3.4	0.8	35	5	111	Present work
MAGS(B)	Sb(V)	3.4	0.8	35	5	125	Present work
Acid-treated cyanobacteria	Sb(V)	2.5-2.6	50	room temperature	2	9.61	23
Zr(IV)-loaded SOW*	Sb(V)	2.5	1.67	30	24	145	26
Fe(III)-loaded SOW	Sb(V)	2.5	1.67	30	24	145	26
Kaolinite	Sb(V)	6	25	50	24	16.3	24
α-FeOOH	Sb(V)	4	0.4	20.5	24	24.5	27
β-FeOOH	Sb(V)	4	0.4	20.5	24	29.2	27
γ-FeOOH	Sb(V)	4	0.4	20.5	24	34.1	27
α-Fe$_2$O$_3$	Sb(V)	4	0.4	20.5	24	23.4	27
HFO**	Sb(V)	4	0.4	20.5	24	114	27

*Saponified orange waste; ** Hydrous ferric oxide.
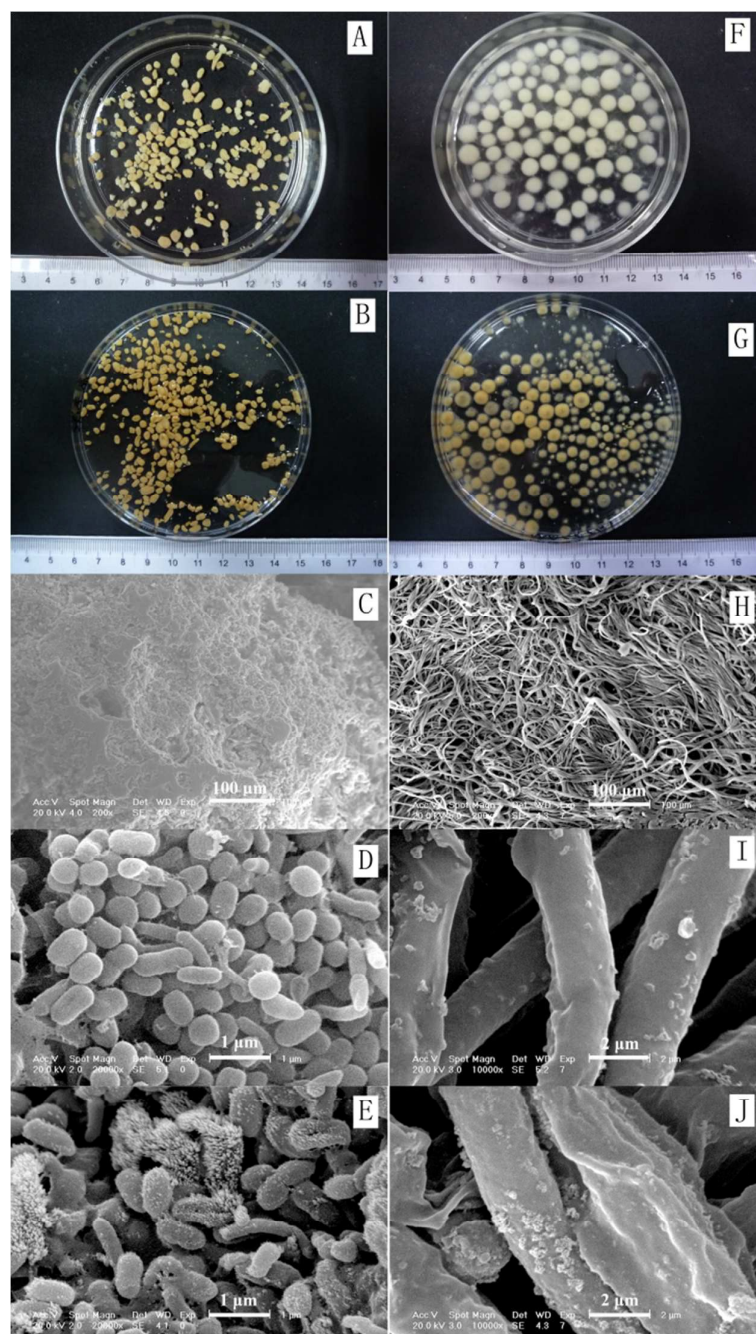
Fig. 1. Morphology observations of the bacterial and fungal granules. (A) original bacterial granules (B) Fe(III) modified bacterial granules; (C) original bacterial granules surface; (D) original bacterial granules surface (detailed); (E) bacterial granules surface after modification; (F) original fungal granules; (G) Fe(III) modified fungal granules; (H) original fungal granules surface; (I) original fungal granules surface (detailed); (J) fungal granules surface after modification.
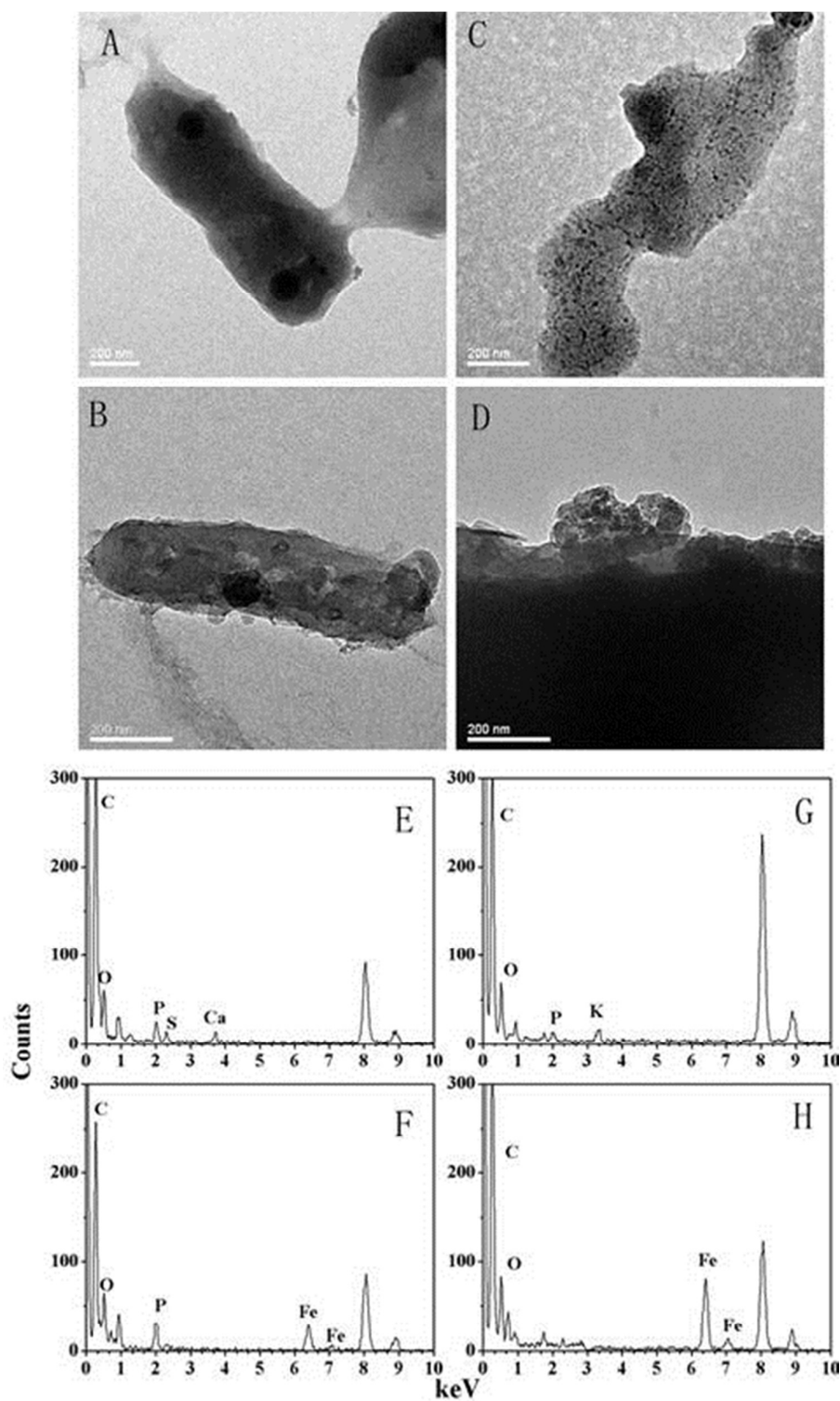
Fig. 2. TEM images and EDS spectra of bacterial and fungal granules. (A) original bacterial granules; (B) modified bacterial granules; (C) original fungal granules; (D) modified fungal granules; (E), (F), (G) and (H) were the corresponding EDS spectra.
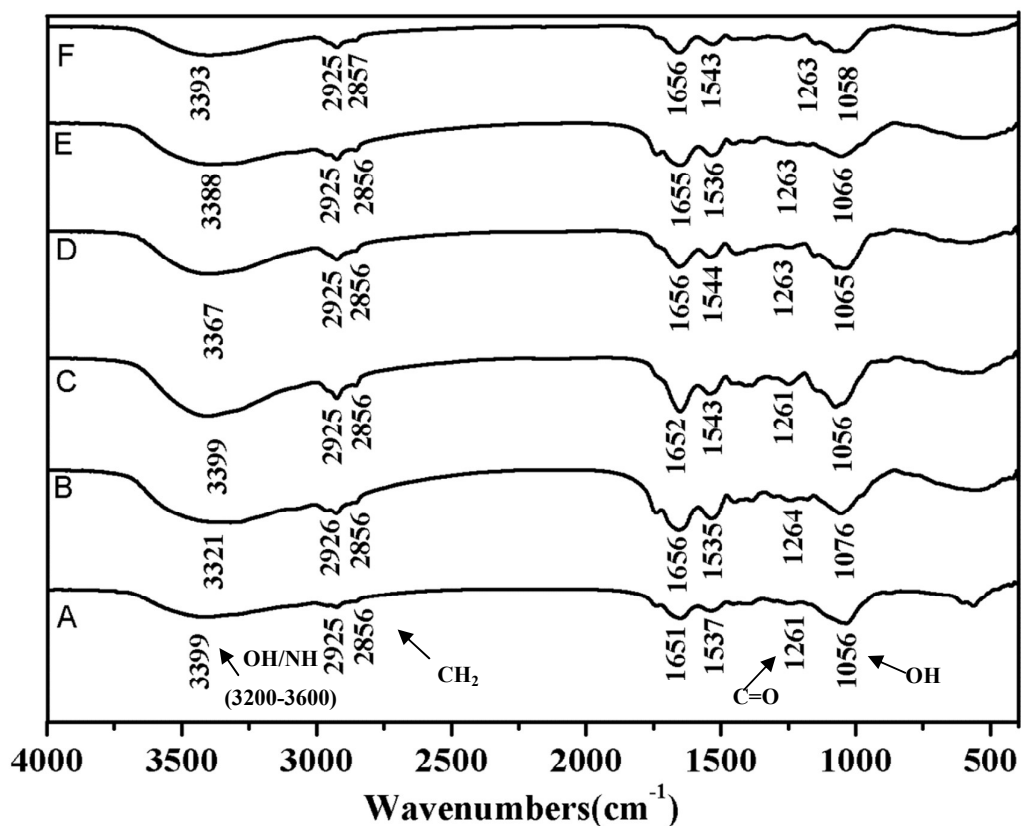
Fig. 3. FTIR spectra of (A) original bacterial granules; (B) modified bacterial granules; (C) original fungi granules; (D) modified fungi granules; (E) modified bacterial granules after Sb adsorption; (F) modified fungi granules after Sb adsorption.
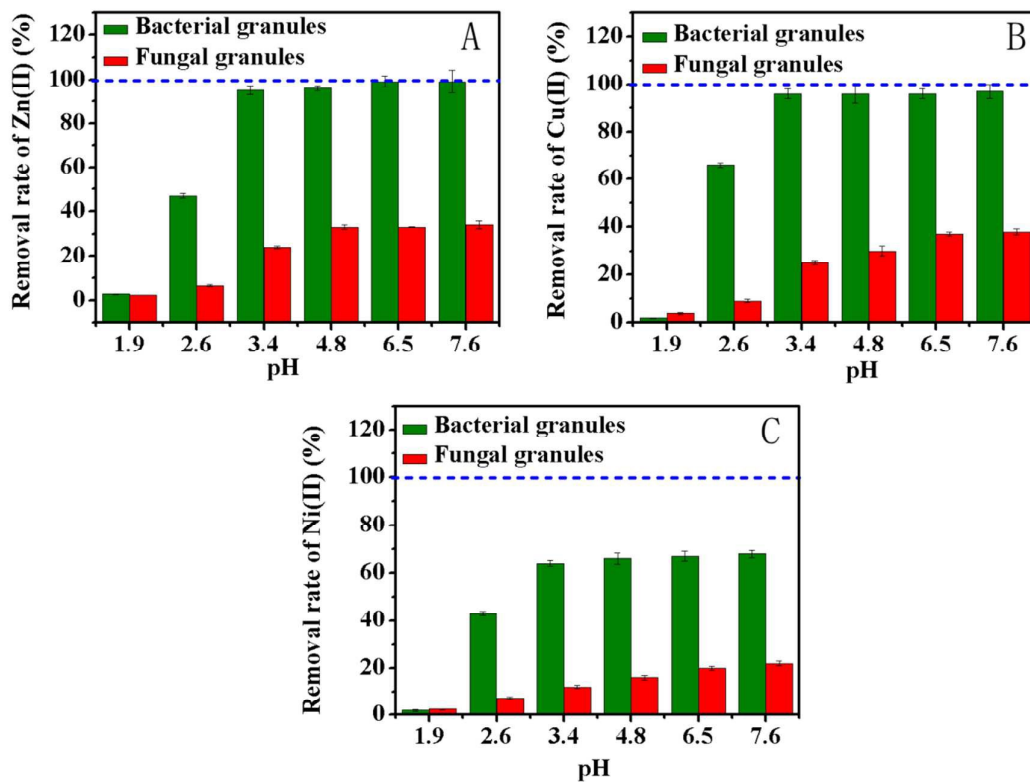
Fig. 4. Removal percentages of cationic metals by original bacterial and fungal granules. (A) Zn(II); (B) Cu(II); (C) Ni(II); (T: 35 ^{o}C, shake speed: 175 rpm, C_0 of the ions: 10 mg L^{-1}, granule dosage: 0.6 g L^{-1}).
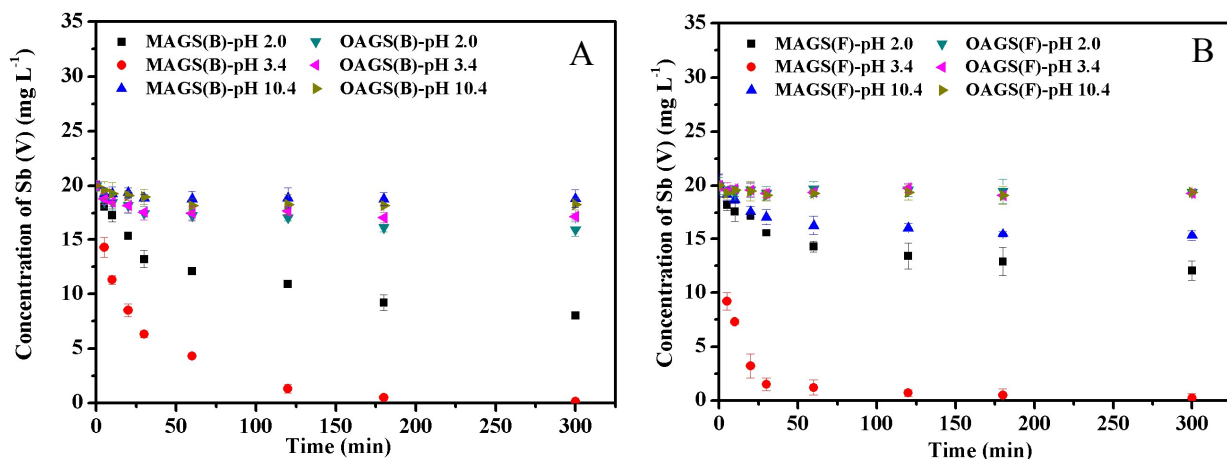
Fig. 5. The effect of pH on Sb(V) removal by (A) original and modified bacterial granules and (B) original and modified fungi granules with time; (T: 35 ^{o}C, shake speed: 175 rpm, C_0 of the ions: 20 mg L^{-1}, biomass dosage: 1 g L^{-1}).
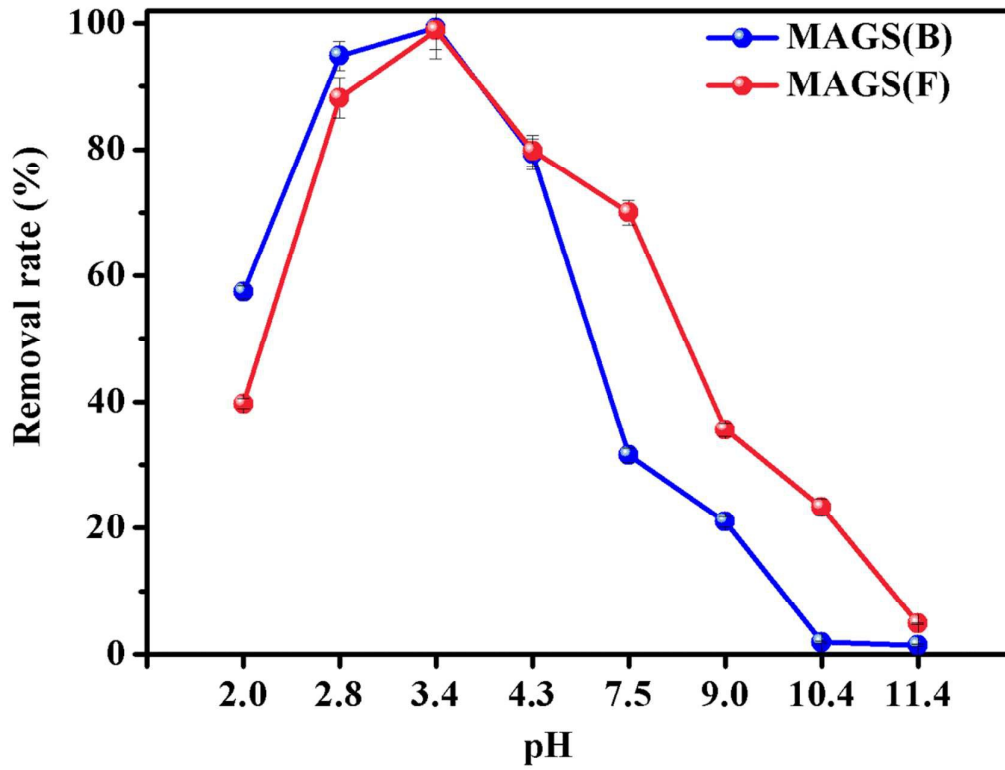
Fig. 6. Effect of pH on Sb(V) removal by modified bacterial and fungal granules; (T:

35 ^{o}C, shake speed: 175 rpm, C_0 of the ions: 20 mg L^{-1}, biomass dosage: 1 g L^{-1}).
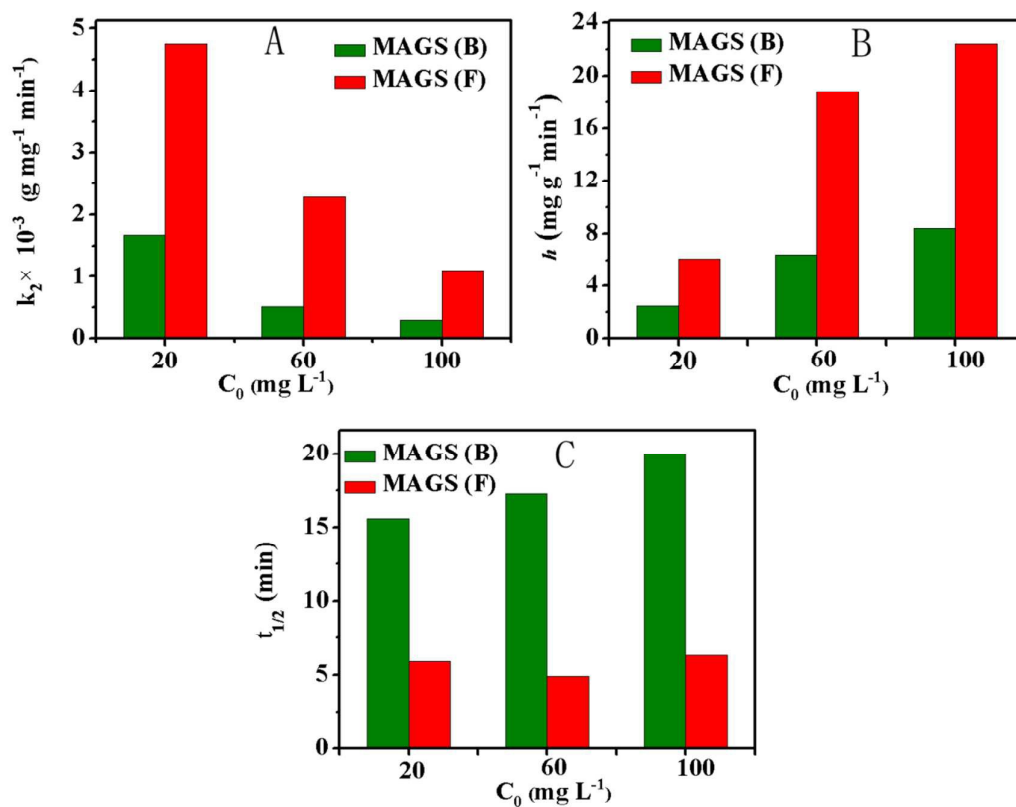
Fig. 7. Comparison of sorption rates by modified bacterial and fungal granules as a function of initial Sb(V) concentrations. (A) Adsorption rate constant; (B) Initial sorption rate constant; (C) Half-adsorption time; (T: 35 ^{o}C, shake speed: 175 rpm, C_0 of the ions: 20 mg L^{-1}, biomass dosage: 0.4 g L^{-1}).